Centrum voor Wiskunde en Informatica
Centre for Mathematics and Computer Science

B. Koren

Low-diffusion rotated upwind schemes, multigrid and defect correction for steady, multi-dimensional Euler flows

Department of Numerical Mathematics Report NM-R9021 November

The Centre for Mathematics and Computer Science is a research institute of the Stichting Mathematisch Centrum, which was founded on February 11, 1946, as a nonprofit institution aiming at the promotion of mathematics, computer science, and their applications. It is sponsored by the Dutch Government through the Netherlands Organization for the Advancement of Research (N.W.O.).

Low-Diffusion Rotated Upwind Schemes, Multigrid and Defect Correction for Steady, Multi-Dimensional Euler Flows

Barry Koren
Centre for Mathematics and Computer Science
P.O. Box 4079, 1009 AB Amsterdam, The Netherlands

Two simple, multi-dimensional upwind discretizations for the steady Euler equations are derived, with the emphasis lying on both a good accuracy and a good solvability. The multi-dimensional upwinding consists of applying a one-dimensional Riemann solver with a locally rotated left and right state, the rotation angle depending on the local flow solution. First, a scheme is derived for which smoothing analysis of point Gauss-Seidel relaxation shows that despite its rather low numerical diffusion, it still enables a good acceleration by multigrid. Next, a scheme is derived which has not any numerical diffusion in crosswind direction, and of which convergence analysis shows that its corresponding discretized equations can be solved efficiently by means of defect correction iteration with in the inner multigrid iteration the first scheme. For the steady, two-dimensional Euler equations, numerical experiments are performed for some supersonic test cases with an oblique contact discontinuity. The numerical results are in good agreement with the theoretical predictions. Comparisons are made with results obtained by standard, grid-aligned upwind schemes. The grid-decoupled results obtained are promising.

1980 Mathematics Subject Classification: 35L65, 35L67, 65N05, 65N10, 76Jxx.
Key Words and Phrases: steady Euler equations, supersonic flows, multi-dimensional upwind schemes, multigrid iteration, defect correction iteration.
Note: This work was supported by the European Space Agency, through Avions Marcel Dassault - Bréguet Aviation. It has been presented at the *Third European Conference on Multigrid Methods*, Bonn, October 1-4, 1990.

1. Introduction

Many upwind schemes used in multi-dimensional (multi-D) flow computations are based on the application of some one-dimensional (1-D) shock capturing scheme in a grid-aligned, direction-split manner. Despite the rigorous mathematics involved in these 1-D upwind schemes, in most multi-D flow computations, the underlying 1-D upwind results are just superposed without any (equally) rigorous mathematical justification. Besides this inconsistency in methodology, the grid-alignment (i.e. grid-dependency) is inconsistent with the upwind principle that discretizations should be dependent on the solution only. Yet, for many practical purposes, very satisfactory results are obtained by applying the direction-split 1-D upwind approach. However, sometimes the aforementioned flaws become clearly visible. In particular, the resolution of layers which are not aligned with the grid may be insufficient. Changing from one shock capturing scheme to another (for instance from some flux splitting scheme to some flux difference splitting scheme) usually does not help in these cases. Simply lowering the magnitude of false diffusion by raising the order of accuracy of the underlying 1-D upwind scheme may help, but possibly at a very high increase in computational cost.

A proper balance needs to be found between both (multi-D) accuracy and solvability. To achieve such a balance, one needs not just control false diffusion's magnitude, but - separately - both its magnitude and its direction. A way to do this is to no longer ignore the multi-D nature of a multi-D flow in the upwind scheme itself. Several grid-decoupled, multi-D upwind discretizations have been published already and many are still in development, a development which is at a rapid pace now. Two main types of multi-D upwind schemes may be considered: (i) those which perform e.g. two flux computations per cell face, the main flux computation upwind in some dominant convection direction and the remaining one e.g. central in a direction normal to that (see e.g. [2,15]), and (ii) those schemes which (try to) transform the Euler equations into a set of decoupled partial differential equations and next apply some well-developed upwind scheme for scalar equations (see e.g. [10,17]).

Report NM-R9021
Centre for Mathematics and Computer Science
P.O. Box 4079, 1009 AB Amsterdam, The Netherlands

Though the emphasis in most multi-D upwind research clearly lies on a good accuracy, some work has also been directed already towards a good efficiency, even some multigrid work. An example of multigrid work in the context of explicit time stepping schemes is that of Catalano and Deconinck [1]. For a 2-D advection equation, Catalano and Deconinck optimize both the stability and the smoothing of an explicit, multi-stage time stepping scheme. As far as we know, the only implicit multigrid work for multi-D upwind discretizations is that performed by Sidilkover [18]. Sidilkover considers steady equations, and solves those directly. A direct multigrid solution approach applied to steady, multi-D upwind discretizations is more ambitious than the equivalent approaches which have been developed for steady, direction-split upwind discretizations (see e.g. [4,9,11]). Multi-D upwinding inherently leads to a greater sensitivity to noise and hence less robustness. Though Sidilkover does not show results of numerical experiments performed for real flow equations (such as e.g. the Euler equations), but - instead - still confines himself to rather simple model equations, from a viewpoint of both accuracy and efficiency, the numerical results presented in [18] are promising. They show that it is worthwhile to investigate direct multigrid methods for multi-D upwind discretizations of the steady Euler equations.

Our aim is to develop for the steady, 2-D Euler equations, in a cell-centered finite volume context: a multi-D upwind method with some appropriate balance between crosswind diffusion and efficiency. The steady equations will be solved directly. Herewith, for obtaining a good efficiency, we rely on nonlinear multigrid (multigrid-Newton) iteration. As the smoothing technique for the multigrid iteration, we prefer to apply point Gauss-Seidel relaxation, using the exact differential matrices (exact Newton). The latter requires the cell face fluxes to be continuously differentiable. If multigrid does not easily meet our standards, we will not try to repair it, but - instead - we will rely on defect correction iteration as an additional iteration. The multi-D upwind schemes to be considered here will be very simple schemes only. They will use neither decoupling of the Euler equations (as in [10,17]), nor rotated fluxes (as in [2,15]). The schemes will be based on *rotated left and right states solely*. Per cell face, just as with the grid-aligned schemes, only a single numerical flux is computed: that normal to the cell face. The numerical flux function to be applied should allow a good resolution of both oblique shock waves and oblique contact discontinuities, fixing choices to flux difference splitting schemes. Given the good experience with Osher's scheme [16] in combination with multigrid - (exact) Newton [9], here we will apply the latter flux difference splitting scheme.

The contents of the paper is as follows. First, in section 2, to set a frame of reference, on the basis of a linear, scalar model equation, an accuracy analysis and a simple solvability analysis are performed for the standard, grid-aligned first-order upwind scheme. Then, two multi-D upwind schemes are derived. Next, in section 3, on the basis of the same model equation, solvability properties of the two schemes derived in section 2 are investigated by Fourier analyses. Finally, in section 4, the theoretical results found in the previous sections are verified for some steady, fully supersonic Euler flows on the unit square.

2. Derivation of grid-decoupled upwind schemes

We will try to derive positive, grid-decoupled upwind schemes which have a low crosswind diffusion (preferably zero), and which (hopefully) still have enough artificial diffusion in characteristic direction to preserve good solvability. An important property required from these schemes is that their stencils are as compact as possible. The motivation for compactness is to avoid: non-consistent boundary condition treatments and - if possible - non-positivity. Compactness will result in a close relationship with the grid-aligned first-order upwind scheme, which therefore will be used as the main reference for comparison. Another property strived for is continuous differentiability, this because of the intended application of exact Newton iteration. The schemes will be investigated on the basis of the linear, scalar, 2-D model equation

$$\cos\phi\frac{\partial u}{\partial x}+\sin\phi\frac{\partial u}{\partial y}=0, \quad 0\leqslant\phi\leqslant\pi/2, \tag{2.1}$$

with ϕ the angle made by the characteristic direction and the x-axis (Fig. 2.1a). Discretization of (2.1) on a square, cell-centered finite volume grid yields

$$\cos\phi(u_{i+\frac{1}{2},j}-u_{i-\frac{1}{2},j})+\sin\phi(u_{i,j+\frac{1}{2}}-u_{i,j-\frac{1}{2}})=0, \tag{2.2}$$

where the non-integer indices refer to the cell faces in between the (integer-indexed) cell centers (Fig. 2.1b).

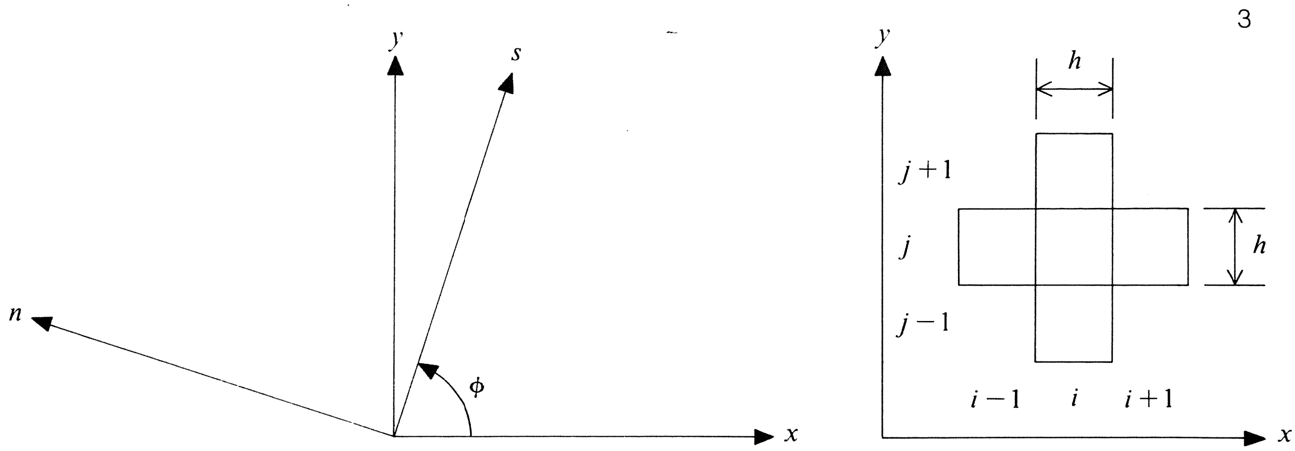

a. Angle characteristic direction and characteristic coordinates.

b. Square finite volume i,j with neighbors.

Fig. 2.1. Geometric situation.

In the grid-aligned first-order upwind scheme, given the being positive of $\cos\phi$ and $\sin\phi$, for the cell face states we take

$$\begin{bmatrix} u_{i+\frac{1}{2},j} \\ u_{i,j+\frac{1}{2}} \end{bmatrix} = \begin{bmatrix} u_{i,j} \\ u_{i,j} \end{bmatrix}, \quad 0 \leqslant \phi \leqslant \pi/2. \tag{2.3}$$

Similar choices are made for $u_{i-\frac{1}{2},j}$ and $u_{i,j-\frac{1}{2}}$. Substituting these cell face states into (2.2) and applying next truncated Taylor series expansions, the following modified equation may be derived:

$$\cos\phi\frac{\partial u}{\partial x} + \sin\phi\frac{\partial u}{\partial y} - \frac{h}{2}\left[\cos\phi\frac{\partial^2 u}{\partial x^2} + \sin\phi\frac{\partial^2 u}{\partial y^2}\right] = O(h^2), \quad 0 \leqslant \phi \leqslant \pi/2. \tag{2.4}$$

By transformation to characteristic coordinates (Fig. 2.1a), (2.4) becomes

$$\frac{\partial u}{\partial s} - \frac{h}{2}\left[(\cos^3\phi + \sin^3\phi)\frac{\partial^2 u}{\partial s^2} - 2\cos\phi\sin\phi(\cos\phi - \sin\phi)\frac{\partial^2 u}{\partial s\partial n} + \right.$$
$$\left. \cos\phi\sin\phi(\cos\phi + \sin\phi)\frac{\partial^2 u}{\partial n^2}\right] = O(h^2), \quad 0 \leqslant \phi \leqslant \pi/2. \tag{2.5}$$

From (2.5) now, it appears that for the grid-aligned first-order upwind scheme, zero-crosswind diffusion (i.e. both $\cos\phi\sin\phi(\cos\phi-\sin\phi)=0$ and $\cos\phi\sin\phi(\cos\phi+\sin\phi)=0$) occurs only in case of $\phi=0$ or $\phi=\pi/2$, i.e. in case of grid-alignment of the characteristic direction. For the sake of comparisons to be made hereafter, in Fig. 2.2a we give the distributions of the diffusion coefficients from (2.5), over the complete range of ϕ considered. In here and also in the following, μ_{ss}, μ_{sn} and μ_{nn} denote the coefficients of $\partial^2 u/\partial s^2$, $\partial^2 u/\partial s\partial n$ and $\partial^2 u/\partial n^2$, respectively.

As opposed to the poor accuracy properties, the smoothing properties of point Gauss-Seidel relaxation applied to the grid-aligned first-order upwind system are known to be good. The fact that these smoothing properties are at least not bad is reflected by the fact that the discretization is positive, which clearly appears from the stencil

$$\begin{array}{c|c|c|} j & -\cos\phi & \cos\phi+\sin\phi \\ \cline{2-3} j-1 & & -\sin\phi \\ \cline{3-3} & i-1 & i \end{array}, \quad 0 \leqslant \phi \leqslant \pi/2\,. \tag{2.6}$$

2.1. A positive, continuously differentiable scheme

The most compact, grid-decoupled upwind schemes use

$$\begin{bmatrix} u_{i+\frac{1}{2},j} \\ u_{i,j+\frac{1}{2}} \end{bmatrix} = \begin{bmatrix} \delta_1(\phi)u_{i,j} + [1-\delta_1(\phi)]u_{i,j-1} \\ \delta_2(\phi)u_{i,j} + [1-\delta_2(\phi)]u_{i-1,j} \end{bmatrix}, \quad 0 \leqslant \delta_1(\phi), \delta_2(\phi) \leqslant 1, \quad 0 \leqslant \phi \leqslant \pi/2. \tag{2.7}$$

The coefficients $\delta_1(\phi)$ and $\delta_2(\phi)$, whose choice determines the scheme, are taken in the range [0,1] in order to prevent unphysical features such as e.g. a negative density. The stencil corresponding with (2.7) reads

$$\begin{array}{c|c|c|} & -\delta_1\cos\phi+(1-\delta_2)\sin\phi & \delta_1\cos\phi+\delta_2\sin\phi \\ j & & \\ j-1 & -(1-\delta_1)\cos\phi-(1-\delta_2)\sin\phi & (1-\delta_1)\cos\phi-\delta_2\sin\phi \\ & i-1 & i \end{array}, \quad 0\leqslant\phi\leqslant\pi/2. \tag{2.8}$$

A natural requirement imposed to the discretization is that of symmetry with respect to $\phi=\pi/4$; in formula:

$$\delta_2(\phi)=\delta_1(\pi/2-\phi), \quad 0\leqslant\phi\leqslant\pi/2. \tag{2.9}$$

Notice that the grid-aligned first-order upwind stencil (2.6) is also covered by (2.7) and (2.9); it is obtained by simply taking $\delta_1(\phi)=1$, $\delta_2(\phi)=1$, $0\leqslant\phi\leqslant\pi/2$.
The modified equation corresponding with (2.7) reads in characteristic coordinates

$$\frac{\partial u}{\partial s}-\frac{h}{2}\Bigg[\Big[(1+\cos\phi\sin\phi)(\cos\phi+\sin\phi)-2(\delta_1\cos\phi+\delta_2\sin\phi)\cos\phi\sin\phi\Big]\frac{\partial^2 u}{\partial s^2}+$$
$$2(\cos\phi-\sin\phi)\Big[1+\cos\phi\sin\phi-(\delta_1\cos\phi+\delta_2\sin\phi)(\cos\phi+\sin\phi)\Big]\frac{\partial^2 u}{\partial s\partial n}+$$
$$2\cos\phi\sin\phi\Big[(\delta_1-\tfrac{1}{2})\cos\phi+(\delta_2-\tfrac{1}{2})\sin\phi\Big]\frac{\partial^2 u}{\partial n^2}\Bigg]=O(h^2), \quad 0\leqslant\phi\leqslant\pi/2. \tag{2.10}$$

Following (2.10), $\mu_{sn}=0$ and $\mu_{nn}=0$ lead to respectively

$$\delta_1\cos\phi+\delta_2\sin\phi=\frac{1+\cos\phi\sin\phi}{\cos\phi+\sin\phi}, \quad 0\leqslant\phi\leqslant\pi/2, \tag{2.11a}$$

$$\delta_1\cos\phi+\delta_2\sin\phi=\tfrac{1}{2}(\cos\phi+\sin\phi), \quad 0\leqslant\phi\leqslant\pi/2, \tag{2.11b}$$

which clearly is an inconsistent system of equations, leading to the following theorem:

THEOREM (2.1)
No most compact grid-decoupled upwind scheme exists for which both $\mu_{sn}=0$ and $\mu_{nn}=0$.

Next, concerning crosswind diffusion, we only require μ_{nn} to be zero, i.e. we assume (2.11b) to hold solely. Further, following (2.8), positivity can be expressed as:

$$(\delta_1\cos\phi+\delta_2\sin\phi)\begin{pmatrix}1\\1\\1\\-1\end{pmatrix}>\begin{pmatrix}0\\ \sin\phi\\ \cos\phi\\ -\cos\phi-\sin\phi\end{pmatrix}, \quad 0\leqslant\phi\leqslant\pi/2. \tag{2.12}$$

It appears that the system (2.11b)-(2.12) is inconsistent as well, leading to the theorem:

THEOREM (2.2)
No most compact grid-decoupled upwind scheme exists which is positive and for which $\mu_{nn}=0$.

Finally, we require $\mu_{sn}=0$ to hold (i.e. (2.11a)) in combination with (2.12). It can be verified that this system is consistent. Assuming the form $\delta_1(\phi)=(\cos\phi+a\sin\phi)/(\cos\phi+\sin\phi)$, a being a constant, with symmetry requirement (2.9) we get $\delta_2(\phi)=(\sin\phi+a\cos\phi)/(\sin\phi+\cos\phi)$. Substitution of these forms of $\delta_1(\phi)$ and $\delta_2(\phi)$ into (2.11a) yields $a=\tfrac{1}{2}$, so

$$\begin{pmatrix}u_{i+\frac{1}{2},j}\\ u_{i,j+\frac{1}{2}}\end{pmatrix}=\frac{1}{\cos\phi+\sin\phi}\begin{pmatrix}(\cos\phi+\tfrac{1}{2}\sin\phi)u_{i,j}+\tfrac{1}{2}\sin\phi\; u_{i,j-1}\\ (\sin\phi+\tfrac{1}{2}\cos\phi)u_{i,j}+\tfrac{1}{2}\cos\phi\; u_{i-1,j}\end{pmatrix}, \quad 0\leqslant\phi\leqslant\pi/2, \tag{2.13}$$

which gives the (positive) stencil

$$\begin{array}{c|c|c|} j & \dfrac{-\cos^2\phi}{\cos\phi+\sin\phi} & \dfrac{1+\cos\phi\sin\phi}{\cos\phi+\sin\phi} \\ j-1 & \dfrac{-\cos\phi\sin\phi}{\cos\phi+\sin\phi} & \dfrac{-\sin^2\phi}{\cos\phi+\sin\phi} \\ & i-1 & i \end{array}, \quad 0\leqslant\phi\leqslant\pi/2, \tag{2.14}$$

and the modified equation

$$\frac{\partial u}{\partial s}-\frac{h}{2}\left[\frac{1+\cos\phi\sin\phi}{\cos\phi+\sin\phi}\frac{\partial^2 u}{\partial s^2}+\frac{\cos\phi\sin\phi}{\cos\phi+\sin\phi}\frac{\partial^2 u}{\partial n^2}\right]=O(h^2),\quad 0\leqslant\phi\leqslant\pi/2. \tag{2.15}$$

In Fig. 2.2b we give the graph of the present scheme's diffusion properties. The scheme's crosswind diffusion is significantly lower than that of the grid-aligned first-order upwind scheme (Fig. 2.2a). The lower crosswind diffusion in combination with the properties of positivity and continuous differentiability makes that scheme (2.13) is possibly more appropriate for our present multigrid purposes than the grid-aligned first-order upwind scheme (2.3).

2.2. A zero-crosswind diffusion scheme

Because of the limitation of the most compact, grid-decoupled upwind schemes with respect to the elimination of all crosswind diffusion (the limitation expressed by THEOREM (2.1)), in this section, we will consider wider stencils. To start with, we consider a situation with small ϕ. Still striving for compactness, the extrapolation is done from the nearest lines connecting two neighboring cell center states, also avoiding negative coefficients herewith:

$$\begin{pmatrix}u_{i+½,j}\\ u_{i,j+½}\end{pmatrix}=\begin{pmatrix}\delta_1(\phi)u_{i,j}+[1-\delta_1(\phi)]u_{i,j-1}\\ \delta_2(\phi)u_{i-1,j}+[1-\delta_2(\phi)]u_{i-1,j+1}\end{pmatrix},\quad 0\leqslant\delta_1(\phi),\delta_2(\phi)\leqslant 1,\quad 0\leqslant\phi\leqslant\phi_{up}, \tag{2.16}$$

with the (small) upper bound ϕ_{up} not yet fixed. With (2.16), we find the following modified equation

$$\frac{\partial u}{\partial s}-\frac{h}{2}\Bigg[\left(\cos^3\phi+2(1-\delta_1)\cos^2\phi\sin\phi+2\cos\phi\sin^2\phi+(2\delta_2-1)\sin^3\phi\right)\frac{\partial^2 u}{\partial s^2}+$$
$$2\left((1-\delta_1)\cos^3\phi+(\delta_1+2\delta_2-2)\cos\phi\sin^2\phi-\sin^3\phi\right)\frac{\partial^2 u}{\partial s\partial n}+$$
$$\cos\phi\sin\phi\left((2\delta_1+2\delta_2-3)\cos\phi-\sin\phi\right)\frac{\partial^2 u}{\partial n^2}\Bigg]=O(h^2),\quad 0\leqslant\phi\leqslant\phi_{up}. \tag{2.17}$$

From this, it follows that no crosswind diffusion occurs for $\delta_1(\phi)=1$, $\delta_2(\phi)=½(1+\tan\phi)$, $0\leqslant\phi\leqslant\pi/4$, where the indicated ϕ-range (with $\phi_{up}=\pi/4$) is that for which negative coefficients are just avoided. Taking for the remaining subrange the symmetrical counterpart of (2.16):

$$\begin{pmatrix}u_{i+½,j}\\ u_{i,j+½}\end{pmatrix}=\begin{pmatrix}\delta_1(\phi)u_{i,j-1}+[1-\delta_1(\phi)]u_{i+1,j-1}\\ \delta_2(\phi)u_{i,j}+[1-\delta_2(\phi)]u_{i-1,j}\end{pmatrix},\quad \pi/4\leqslant\phi\leqslant\pi/2, \tag{2.18}$$

with symmetry condition (2.9) we get $\delta_1(\phi)=½(1+\text{cotan}\phi)$, $\delta_2(\phi)=1$, $\pi/4\leqslant\phi\leqslant\pi/2$. Summarizing, we have derived as expressions for the cell face states:

$$\begin{pmatrix}u_{i+½,j}\\ u_{i,j+½}\end{pmatrix}=\begin{pmatrix}u_{i,j}\\ ½(1+\tan\phi)u_{i-1,j}+½(1-\tan\phi)u_{i-1,j+1}\end{pmatrix},\quad 0\leqslant\phi\leqslant\pi/4, \tag{2.19a}$$

$$\begin{pmatrix}u_{i+½,j}\\ u_{i,j+½}\end{pmatrix}=\begin{pmatrix}½(1+\text{cotan}\phi)u_{i,j-1}+½(1-\text{cotan}\phi)u_{i+1,j-1}\\ u_{i,j}\end{pmatrix},\quad \pi/4\leqslant\phi\leqslant\pi/2, \tag{2.19b}$$

as corresponding stencils:

	$i-1$	i
$j+1$	$½\sin\phi(1-\tan\phi)$	
j	$\sin\phi(\tan\phi-\text{cotan}\phi)$	$\cos\phi$
$j-1$	$-½\sin\phi(1+\tan\phi)$	

$, \quad 0\leqslant\phi\leqslant\pi/4,$ (2.20a)

	$i-1$	i	$i+1$
j		$\sin\phi$	
$j-1$	$-½\cos\phi(1+\text{cotan}\phi)$	$\cos\phi(\text{cotan}\phi-\tan\phi)$	$½\cos\phi(1-\text{cotan}\phi)$

$, \quad \pi/4\leqslant\phi\leqslant\pi/2,$ (2.20b) and as modified equations:

$$\frac{\partial u}{\partial s}-\frac{h}{2}\frac{1}{\cos\phi}\frac{\partial^2 u}{\partial s^2}=O(h^2),\quad 0\leqslant\phi\leqslant\pi/4, \tag{2.21a}$$

$$\frac{\partial u}{\partial s}-\frac{h}{2}\frac{1}{\sin\phi}\frac{\partial^2 u}{\partial s^2}=O(h^2),\quad \pi/4\leqslant\phi\leqslant\pi/2. \tag{2.21b}$$

A geometric interpretation of scheme (2.19) is given in [8]. In Fig. 2.2c, we give the graph with its diffusion coefficients. Unfortunately, from (2.20) it appears that the scheme is non-positive. A favorable property of the scheme is its simplicity.

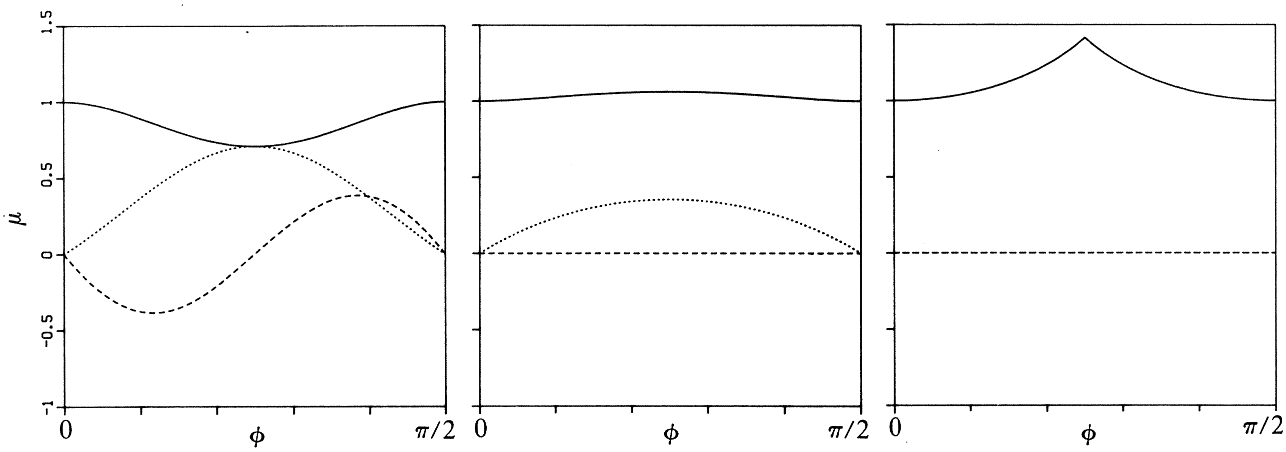

a. Grid-aligned first-order upwind scheme (2.3).

b. Continuously differentiable scheme (2.13).

c. Zero-crosswind diffusion scheme (2.19).

Fig. 2.2. Diffusion coefficients modified equation (μ_{ss}: ——, μ_{sn}: ------, μ_{nn}: ··········).

3. Performance analysis of multigrid iteration and defect correction iteration

In the foregoing section, two promising, grid-decoupled upwind schemes have been derived; one being positive, the other being non-positive, both being compact. The positive scheme; scheme (2.13), is most compact, continuously differentiable, low-diffusive in crosswind direction, and - possibly - still enough diffusive in both crosswind and characteristic direction to allow a good smoothing of point Gauss-Seidel relaxation and hence a successful application of multigrid iteration. The non-positive scheme; scheme (2.19), is zero-diffusive in crosswind direction and hence most promising from the viewpoint of accuracy. Probably, its corresponding discretized equations cannot be solved efficiently by means of multigrid iteration, with point Gauss-Seidel relaxation as the smoother.

In the present section, we will analyze some possible solution methods. The analyses will be done again for model equation (2.1) on a square, cell-centered finite volume grid. First, the smoothing behavior of point Gauss-Seidel relaxation will be investigated, both for scheme (2.13) and scheme (2.19). (Though we do not expect the latter scheme to be sufficiently dissipative to allow a successful application of multigrid iteration, for sake of certainty we do consider its smoothing behavior.) The smoothing properties found will be compared with those of the grid-aligned first-order upwind scheme.

If analysis shows that multigrid iteration applied directly to the zero-crosswind diffusion operator does not work, to solve the corresponding system of discretized equations, we will rely on defect correction iteration, with (possibly) positive, continuously differentiable scheme (2.13) as the approximate scheme in the inner multigrid iteration. In [18], Sidilkover objects that defect correction iteration is not a fully efficient solution technique for non-elliptic problems, and he states that he still prefers multigrid solely. To our opinion, for a given grid, multigrid solely does not allow sufficiently accurate solutions, in general it requires too dissipative discretizations. When considering the convergence of defect correction iteration in some general error norm, we agree that for non-elliptic problems, it is not fully efficient. (See e.g. [3] and [7] for respectively some theoretical and experimental evidence on this.) However, considering - instead of the error's convergence to zero - the solution's convergence to higher-order accuracy, one gets a more satisfactory picture, both in theory [5] and in practice [6,12,13].

3.1. Smoothing analysis of point Gauss-Seidel relaxation

Four different relaxation sweep directions are considered: downwind, upwind and twice crosswind, each of those four with the i-loop as the inner sweep-loop, and each of those for the complete range of ϕ considered: $[0,\pi/2]$. To perform smoothing analysis, denoting the number of sweeps performed by n, we introduce: (i) the iteration error

$$\delta_{i,j}^{n} \equiv u_{i,j}^{*} - u_{i,j}^{n}, \tag{3.1}$$

with $u_{i,j}^{*}$ the converged numerical solution in finite volume i,j, and (ii) the Fourier form

$$\delta_{i,j}^{n} = D\rho^{n} e^{\mathrm{i}(\theta_1+\theta_2)}, \tag{3.2}$$

with D constant, ρ the amplification factor, and $\theta_1 \equiv \omega_1 h$ and $\theta_2 \equiv \omega_2 h$, ω_1 and ω_2 being the error mode in i- and j-direction, respectively. In Fig. 3.1, results of the smoothing analysis are given for successively: grid-aligned first-order upwind scheme (2.3), continuously differentiable scheme (2.13) and zero-crosswind diffusion scheme (2.19). In here, the smoothing factor ρ_s is defined as

$$\rho_s \equiv \sup|\rho(\theta_1,\theta_2)|, \quad (|\theta_1|,|\theta_2|) \in \{[0,\pi]\times[0,\pi] \,|\, |\theta_1| \in [\pi/2,\pi] \vee |\theta_2| \in [\pi/2,\pi]\}. \tag{3.3}$$

It appears that the zero-crosswind diffusion scheme does not enable a successful application of multigrid with point Gauss-Seidel relaxation as the smoother (Fig. 3.1c). Notice that even for the corresponding downwind relaxation sweep, smoothing is not guaranteed over the complete range of ϕ considered. As opposed to this, for the positive, continuously differentiable scheme we do have smoothing (Fig. 3.1b).

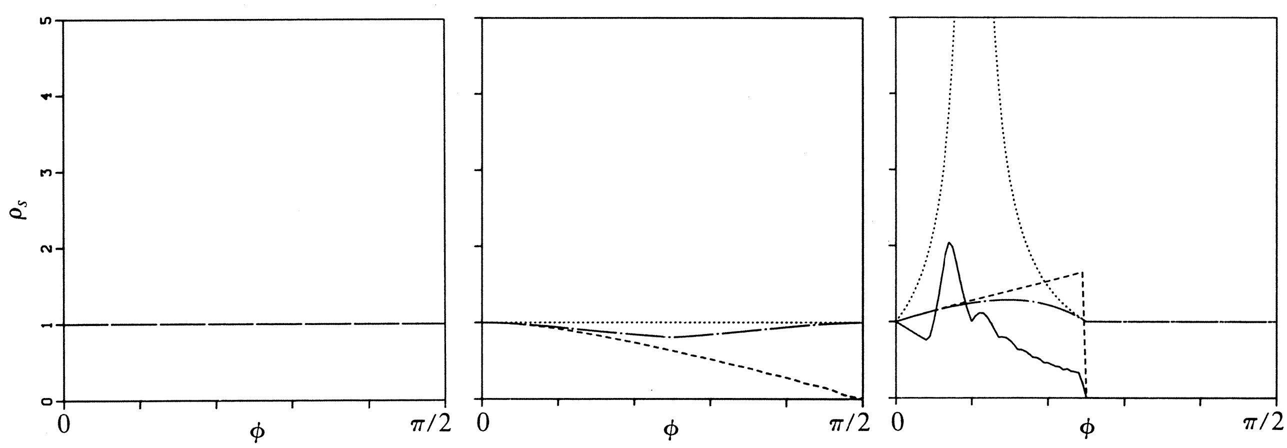

a. Grid-aligned first-order upwind scheme (2.3).

b. Continuously differentiable scheme (2.13).

c. Zero-crosswind diffusion scheme (2.19).

Fig. 3.1. Smoothing factors point Gauss-Seidel relaxation, with i-loop as inner loop (downwind; : ——, upwind; : —·—, crosswind up; : ------, crosswind down; : ··········).

To find a suitable solution method for zero-crosswind diffusion scheme (2.19), in the following, we will study the convergence properties of defect correction iteration with positive, continuously differentiable scheme (2.13) as the approximate scheme in the inner multigrid iteration. For comparison, a similar study will also be made with grid-aligned first-order upwind scheme (2.3) as the approximate scheme.

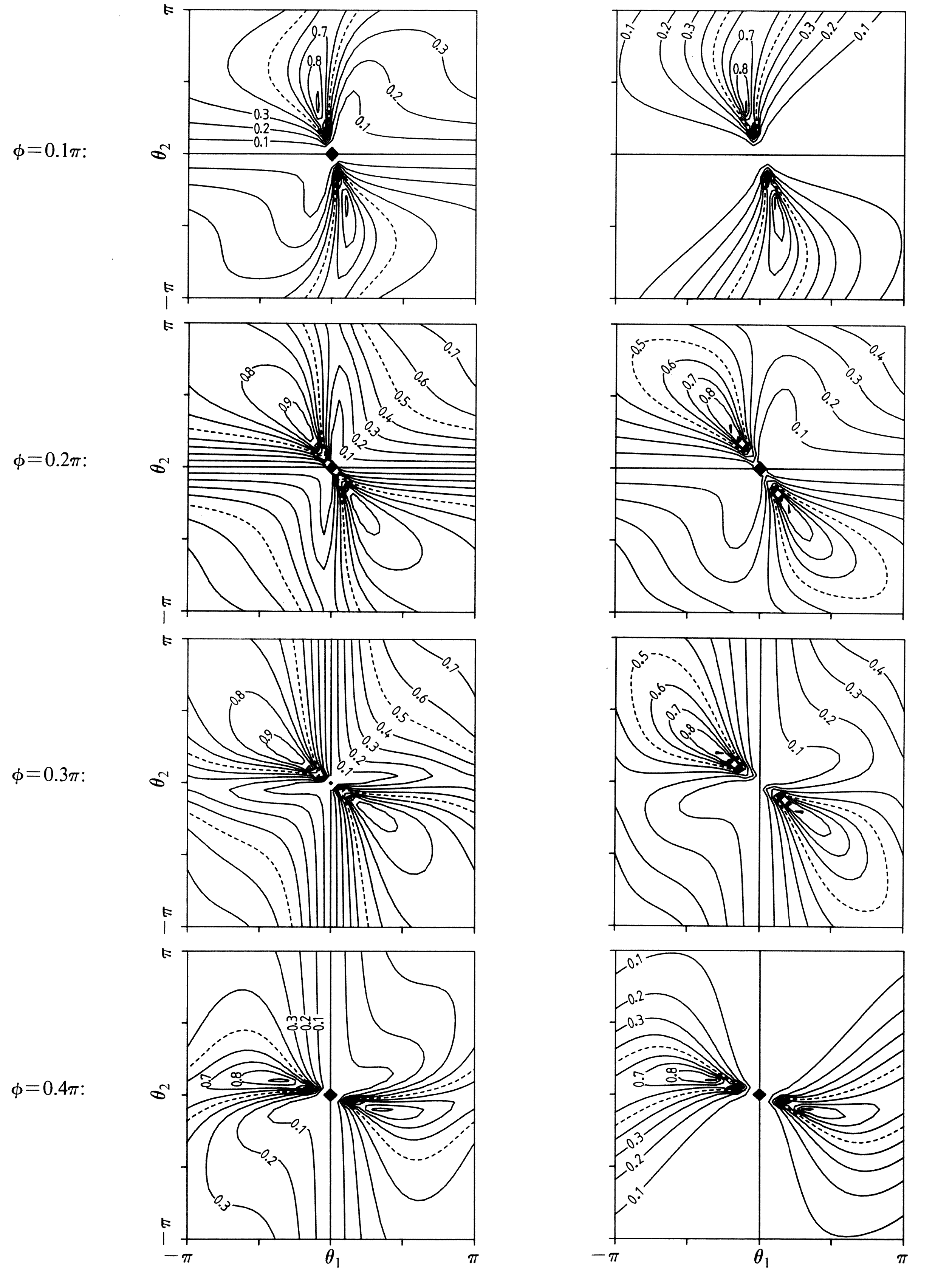

a. Grid-aligned first-order upwind scheme (2.3) as approximate scheme.

b. Continuously differentiable scheme (2.13) as approximate scheme.

Fig. 3.2. Convergence factor distributions defect correction iteration.

3.2. Convergence analysis of defect correction iteration

Denoting the zero-crosswind diffusion operator by L_h^+, defect correction iteration reads

$$L_h(u_h^{n+1}) = L_h(u_h^n) - L_h^+(u_h^n), \quad n = 0,1,...,N, \tag{3.4}$$

with L_h denoting the positive operator to be inverted, and with the index n denoting the iteration counter. From (3.4), it is clear that the closer the resemblance between the target operator L_h^+ and the approximate operator L_h, the better the convergence of the defect correction iteration. Hence, in this respect, the best convergence of (3.4) is expected from the approach with (2.13) as the approximate scheme. Introducing, as before, the iteration error (3.1) in its Fourier form (3.2), we can write for the amplification factor

$$\rho(\theta_1,\theta_2) = 1 - L_h^{-1}(\theta_1,\theta_2)L_h^+(\theta_1,\theta_2). \tag{3.5}$$

In Fig. 3.2, for each of the two approximate schemes (2.3) and (2.13), and for successively $\phi = 0.1\pi, 0.2\pi, 0.3\pi$ and 0.4π, we give the distributions of the convergence factor ρ_c;

$$\rho_c \equiv |\rho(\theta_1,\theta_2)|, \quad (|\theta_1|,|\theta_2|) \in \{[0,\pi]\times[0,\pi]\}. \tag{3.6}$$

In all graphs of Fig. 3.2, the dashed iso-lines correspond with $\rho_c = 0.5$. It appears that, for all four values of ϕ considered, scheme (2.13) as the approximate scheme gives better convergence factor distributions indeed.

4. Numerical results

To investigate some theoretical results found in the previous sections, in this section, for a perfect gas with $\gamma = 1.4$, we perform numerical experiments for a set of fully supersonic Euler flows with oblique contact discontinuity (Fig. 4.1a). The discontinuity is considered for the flow angles $\phi = 0.1\pi, 0.2\pi, 0.3\pi$ and 0.4π. The flows are computed on the 32×32-grid given in Fig. 4.1b. In all cases - for simplicity - at each of the four boundaries, the exact solution is imposed (overspecification). The multigrid method applied for all cases is nonlinear multigrid with V-cycles, and with per level a single pre- and post-relaxation sweep only. In all cases, the coarsest grid considered is a 2×2-grid. Further, in all cases we take as the initial solution: the solution with $q = q^L$ (the q^L from Fig. 4.1a) uniformly constant over the complete domain. For both grid-decoupled upwind schemes derived before, as the angle to be considered at each cell face, we take the streamline angle. In [8], we give a physically proper way of computing this angle.

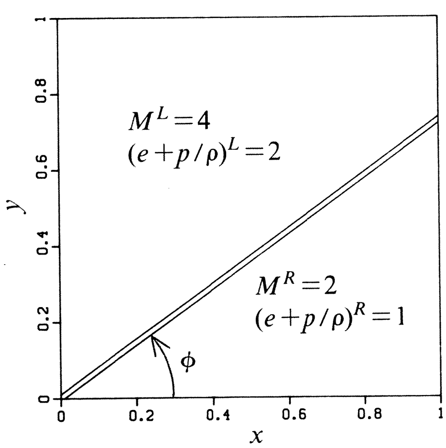

a. Flow with contact discontinuity ($\phi = 0.1\pi, 0.2\pi, 0.3\pi, 0.4\pi$, $p = 1$).

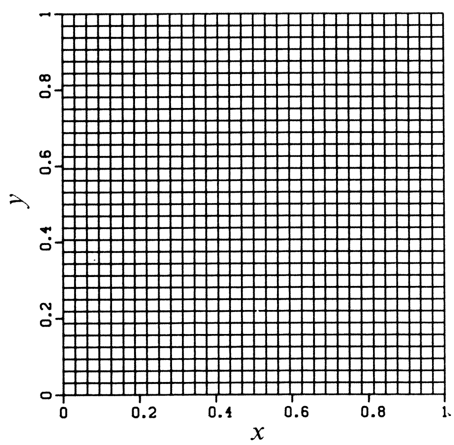

b. Finest grid (32×32).

Fig. 4.1. Test case on unit square.

4.1. Results positive, continuously differentiable scheme

In Fig. 4.2 we first give, on top of each other, the reference results obtained for $\phi=0.1\pi, 0.2\pi, 0.3\pi$ and 0.4π with the grid-aligned first-order upwind scheme; in Fig. 4.2a the multigrid convergence histories and in Fig. 4.2b the enthalpy $(e+p/\rho)$ distributions. The iso-enthalpy values considered in these and all following enthalpy distributions are: $1.1, 1.2, 1.3, \cdots, 1.9$. Because of the severe smearing of the grid-aligned first-order upwind scheme, hardly any distinction can be made between the four solutions. Notice that the layers along $x=1$ and $y=1$, in Fig. 4.2b and all following enthalpy graphs, are only due to the overspecification.

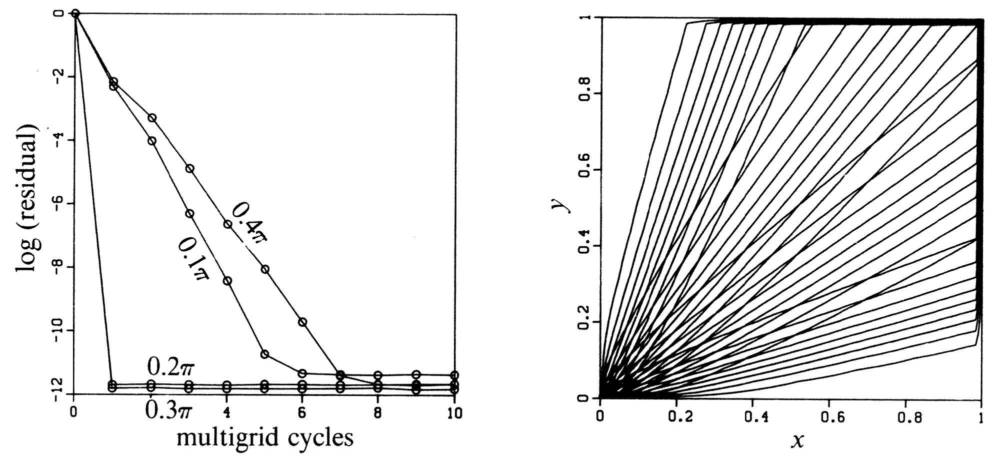

a. Multigrid convergence histories. b. Enthalpy distributions.

Fig. 4.2. Results grid-aligned first-order upwind scheme.

In Fig. 4.3 we give the similar results obtained with the grid-decoupled, positive, continuously differentiable scheme. Though not as very fast as the reference convergence in Fig. 4.2a, fortunately, the present scheme's multigrid convergence is still fast. Though clearly more accurate than the reference distributions in Fig. 4.2b, the present enthalpy distributions are still insufficiently accurate.

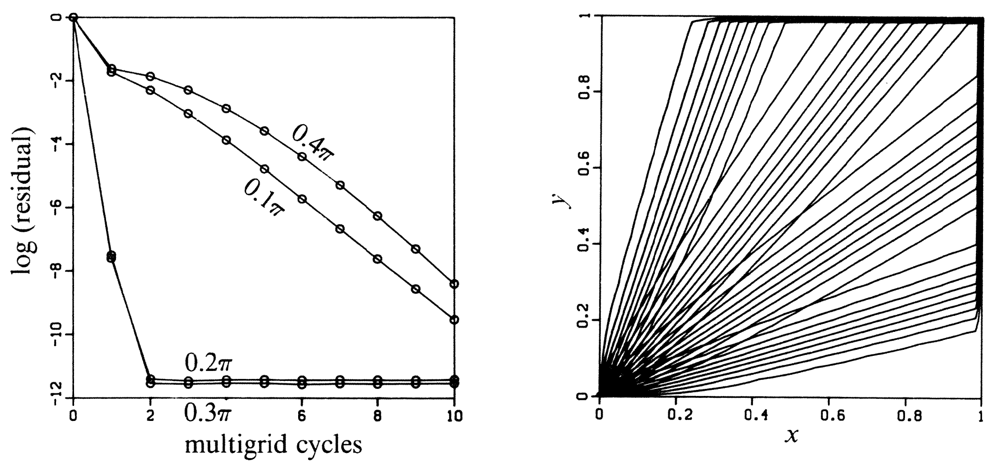

a. Multigrid convergence histories. b. Enthalpy distributions.

Fig. 4.3. Results positive, continuously differentiable scheme.

4.2. Results zero-crosswind diffusion scheme

In Fig. 4.4a we give the enthalpy distributions for the zero-crosswind diffusion scheme, as obtained after 10 defect correction cycles (with per defect correction cycle a single nonlinear multigrid cycle only). As a reference, in Fig. 4.4b we give the distributions obtained with the third-order accurate, grid-aligned $\kappa = 1/3$-scheme [14]. All four enthalpy distributions in Fig. 4.4a appear to be even less diffusive than those of the $\kappa = 1/3$-scheme. Almost in agreement with theory, the distributions in Fig. 4.4a appear to be almost free of crosswind diffusion. Though the being non-positive of the zero-crosswind diffusion scheme allows solutions with spurious oscillations, its distributions are still monotone.

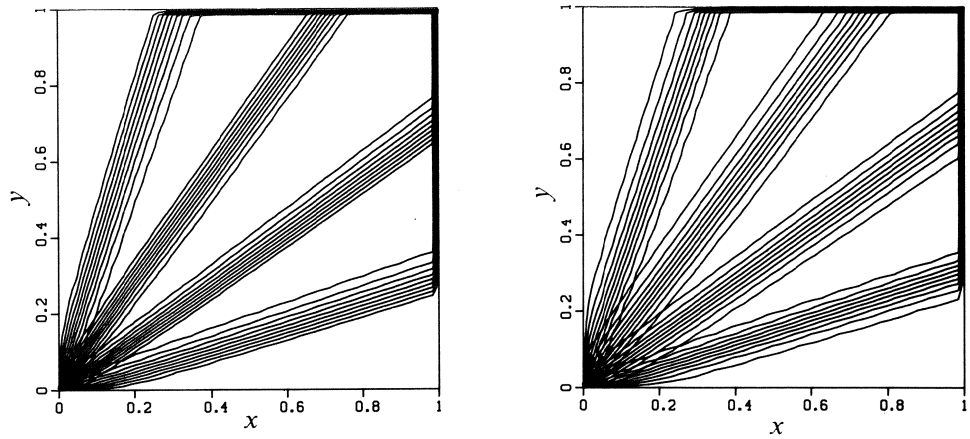

a. Zero-crosswind diffusion scheme. b. $\kappa = 1/3$-scheme.

Fig. 4.4. Enthalpy distributions after 10 defect correction cycles.

An impression of the convergence rate of the defect correction iteration is given in Fig. 4.5. The four distributions in Fig. 4.5a are those of the starting solutions of the defect correction iteration; the solutions of the positive, continuously differentiable scheme after a single multigrid cycle. Notice, as a side-result, the perfect agreement already between these four early distributions and the corresponding distributions as found after 10 multigrid cycles (Fig. 4.3b). Concerning the convergence rate of the defect correction iteration, we are of the opinion that this is good.

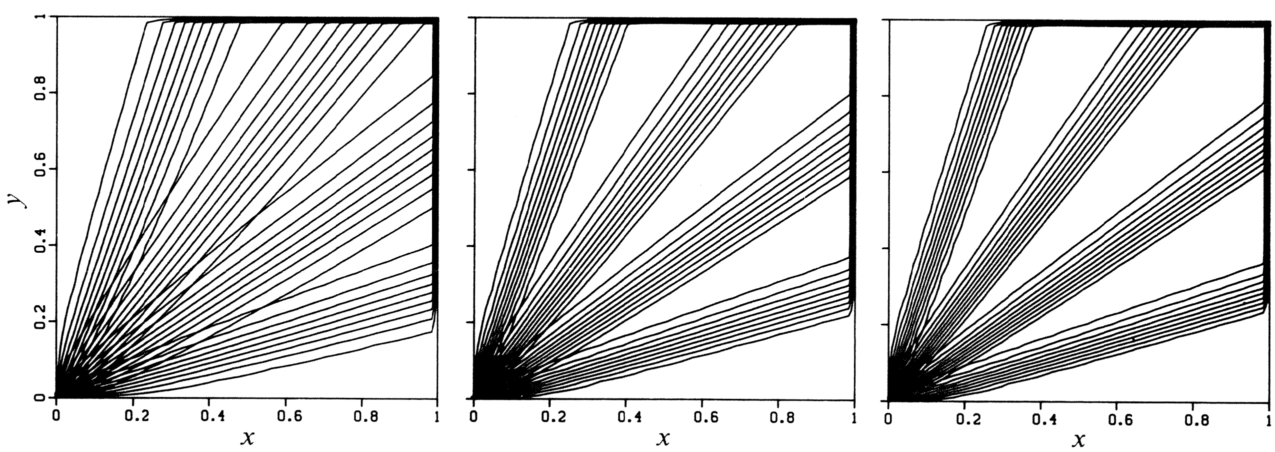

a. Before *1st* cycle. b. After *1st* cycle. c. After *2nd* cycle.

Fig. 4.5. Convergence history defect correction iteration, enthalpy distributions zero-crosswind diffusion scheme.

5. Conclusions

In the present paper, for multi-D Euler equations, two promising multi-D upwind schemes have been derived; a positive, continuously differentiable scheme and a zero-crosswind diffusion scheme. Both scheme9 are based on a one-dimensional Riemann solver. Their multi-D nature is simply realized through a local, solution-dependent rotation of the left and right Riemann state, allowing to keep the number of numerical flux computations per cell face at one only. Good efficiency is strived for by means of nonlinear multigrid iteration and (if necessary) defect correction iteration. The accuracy and efficiency of the numerical results obtained are promising. One important result obtained is that when applying the positive, continuously differentiable scheme, for flows with contact discontinuities, the performance of nonlinear multigrid with point Gauss-Seidel relaxation as the smoother, is very good. Another important result is that, again for flows with contact discontinuities, the solutions of the zero-crosswind diffusion scheme are even less diffused than those of the grid-aligned $\kappa = 1/3$-scheme. Moreover, their computation by means of defect correction iteration (with the grid-decoupled, positive, continuously differentiable scheme as the approximate scheme) is efficient.

References

1. L.A. Catalano and H. Deconinck, *Two-dimensional optimization of smoothing properties of multi-stage schemes applied to hyperbolic equations,* Proceedings of the Third European Conference on Multigrid Methods, Bonn, 1990 (to appear).
2. S.F. Davis, *A rotationally biased upwind difference scheme for the Euler equations,* J. Comput. Phys. 56, 1984, pp. 65-92.
3. J.-A. Desideri and P.W. Hemker, *Analysis of the convergence of iterative implicit and defect-correction algorithms for hyperbolic problems,* Center for Mathematics and Computer Science, Amsterdam, Report NM-R9004, 1990.
4. E. Dick, *A multigrid flux-difference splitting method for steady Euler equations,* Proceedings of the Fourth Copper Mountain Conference on Multigrid Methods, Copper Mountain, CO, 1989, SIAM, Philadelphia, PA, 1989, pp. 117-129.
5. W. Hackbusch, *Multi-Grid methods and applications,* Springer, Berlin, 1985.
6. P.W. Hemker, *Defect correction and higher order schemes for the multi grid solution of the steady Euler equations,* Lecture Notes in Mathematics, No. 1228, Springer, Berlin, 1986, pp. 149-165.
7. P.W. Hemker and B. Koren, *A non-linear multigrid method for the steady Euler equations,* Notes on Numerical Fluid Mechanics, No. 26, Vieweg, Braunschweig, 1989, pp. 175-196.
8. P.W. Hemker, B. Koren and B. van Leer, *Low-diffusion upwind schemes, multigrid and defect correction for steady, multi-dimensional Euler flows,* Center for Mathematics and Computer Science, Amsterdam, NM-Report (in preparation).
9. P.W. Hemker and S.P. Spekreijse, *Multiple grid and Osher's scheme for the efficient solution of the steady Euler equations,* Appl. Numer. Math., 2, 1986, pp. 475-493.
10. Ch. Hirsch, C. Lacor and H. Deconinck, *Convection algorithms based on a diagonalization procedure for the multidimensional Euler equations,* AIAA Paper 87-1163, 1987.
11. D.C. Jespersen, *Design and implementation of a multigrid code for the Euler equations,* Appl. Math. Comput., 13, 1983, pp. 357-374.
12. B. Koren, *Defect correction and multigrid for an efficient and accurate computation of airfoil flows,* J. Comput. Phys., 77, 1988, pp. 183-206.
13. B. Koren, *Multigrid and defect correction for the steady Navier-Stokes equations,* J. Comput. Phys., 87, 1990, pp. 25-46.
14. B. van Leer, *Upwind-difference methods for aerodynamic problems governed by the Euler equations,* Lectures in Applied Mathematics, No. 22, Part 2, American Mathematical Society, Providence, RI, 1985, pp. 327-336.
15. D.W. Levy, K.G. Powell and B. van Leer, *An implementation of a grid-independent upwind scheme for the Euler equations,* AIAA Paper 89-1931, 1989.
16. S. Osher and F. Solomon, *Upwind difference schemes for hyperbolic systems of conservation laws,* Math. Comput., 38, 1982, pp. 339-374.
17. P.L. Roe, *Discrete models for the numerical analysis of time-dependent multi-dimensional gas dynamics,* J. Comput. Phys., 63, 1986, pp. 458-476.
18. D. Sidilkover, *Numerical solution to steady-state problems with discontinuities,* Weizmann Institute of Science, Rehovot, Doctoral Thesis, 1989.